

Radial compression of protons and H_3^+ ions in a multiring trap for the production of ultralow energy antiproton beams

H. Higaki,^{1,*} N. Kuroda,¹ K. Yoshiki Franzen,^{1,†} Z. Wang,^{1,‡} M. Hori,² A. Mohri,³ K. Komaki,¹ and Y. Yamazaki^{1,3}

¹*Institute of Physics, University of Tokyo, 3-8-1, Komaba, Meguro, Tokyo 153-8902 Japan*

²*CERN, CH-1211 Geneva 23, Switzerland*

³*RIKEN, 2-1 Hirosawa, Wako, Saitama 351-0198 Japan*

(Received 13 November 2003; published 24 August 2004)

Radial compression of a proton cloud was performed in a multiring trap which was designed to trap and cool a large number of antiprotons for the production of low-energy (10–1000 eV) antiproton beams. The resonance frequency for the radial compression was almost constant from 3×10^5 to 3×10^6 protons. The collision process of the trapped protons was also investigated to estimate the energy of the protons inside the trap. This technique will be applied to the ASACUSA experiment at the antiproton decelerator, CERN, to extract ultralow antiprotons with good emittance.

DOI: 10.1103/PhysRevE.70.026501

PACS number(s): 41.85.Ar, 41.85.Ct, 41.75.-i, 34.70.+e

I. INTRODUCTION

Pulsed antiproton beams of 10–120 keV are now available from a radio frequency quadrupole decelerator (RFQD) at the antiproton decelerator (AD), CERN. Lower energy antiproton beams are expected to open additional research fields [1,2]. For example, the production of protonium ($p\bar{p}$) in collisions between antiprotons (\bar{p}) and hydrogen atoms (H) is expected to occur for collision energies below 54 eV [3]. However, single collision experiments with antiproton energies lower than 10 keV have not been performed simply because no antiproton beam has been available in this energy range. In order to produce such ultraslow antiproton beams, reacceleration of cold antiprotons from a trap is expected to be a promising method.

In the Atomic Spectroscopy and Collisions Using Slow Antiprotons (ASACUSA) Collaboration [2], electrostatic lenses will be used to extract antiprotons from a strong magnetic field and to focus them into a field-free region where the low-energy antiprotons interact with target particles [4]. Since charged particles tend to follow the magnetic field lines, a cloud of antiprotons should have a small radius in the trap for better focusing of the extracted beam. It is known that sideband cooling is effective in reducing the radius of the magnetron motion of a charged particle in a Penning trap [5]. Also, ion plasmas have been radially compressed in a trap by a rotating electric field [6]. Unfortunately, laser cooling [7] is not applicable to protons and antiprotons. Although various experiments in traps have been conducted so far [8], little attention has been paid to the radial compression of a large number of charged particles in order to extract them from a trap as a beam. It is the purpose of the present paper

to study how charged particles numbering about 10^6 are compressed radially in a multiring trap.

Since the mechanism of radial compression in the trap depends whether the proton cloud is a plasma or not, the proton energy in the trap is an important parameter to be measured. The physical mechanism for the compression must be the same for antiprotons and the same procedure should work equally well for antiprotons. The number of ions handled in this paper is on the order of 10^5 to 10^6 , because the number of antiprotons delivered from the RFQD is about 10^6 antiprotons per one AD shot. Collision processes that take place during the confinement of the protons were also studied to estimate the proton energy.

II. EXPERIMENTAL SETUP

The experimental set up is schematically shown in Fig. 1. The multiring trap is composed of a series of cylindrical electrodes [9]. By applying a proper voltage on each electrode, an electrostatic potential

$$\phi_0(\rho, z) = -V_0(\rho^2 - z^2)/(2L^2 + b^2) + V_b \quad (1)$$

is produced. Here, (ρ, θ, z) are the cylindrical coordinates, $2b=4$ cm the inner diameter of the trap electrode,

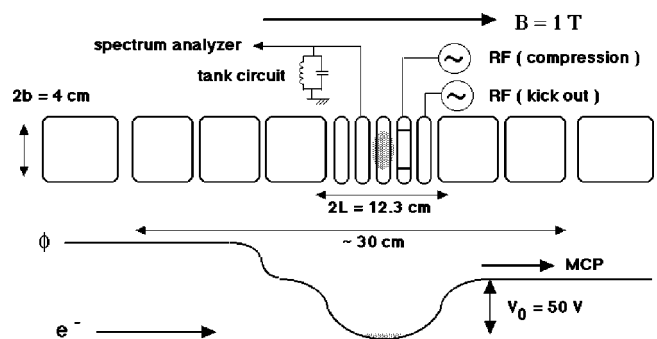


FIG. 1. A schematic of the experimental setup. The external rf electric field for the radial compression of trapped particles is applied through segmented electrodes. The external rf electric field to select the ion species is applied through another ring electrode.

*Present address: Institute of Applied Physics, University of Tsukuba, 1-1-1 Tennoudai, Tsukuba, Ibaraki 305-8571, Japan.

†Present address: LIGO Livingston Observatory, P. O. Box 940, Livingston, LA 70754, USA.

‡Present address: Hitachi High-Technologies Corporation, 882 Icheon, Hitachinaka, Ibaraki, 312-8504 Japan.

$2L=12.3$ cm the axial length of the trap, V_0 the trap depth, and V_b the bias voltage of the trap which controls the energy of the extracted charged particles. In the present experiment, V_0 was 50 V and V_b was varied from -1000 to $+1000$ V. The axial harmonic oscillation frequency of a charged particle with a charge e and a mass M in the trap is given by $f_z = \sqrt{4eV_0/M(2L^2+b^2)}/2\pi$. The trap was immersed in a uniform axial magnetic field $B=10$ kG.

The bore tube housing the trap was cooled to 30 K. The partial residual gas pressure measured outside the cold region was $\approx 7.0 \times 10^{-10}$ torr of H_2 and $\approx 4.5 \times 10^{-11}$ torr of H_2O . In the cooled region, the partial pressure of H_2O should be practically zero. On the other hand, the density of molecular hydrogen is expected to be similar to that outside, i.e., $n_{H_2} \approx 2.5 \times 10^7$ cm $^{-3}$. Since the injection of 10^6 low-energy protons from outside into the trap was not possible with the present experimental setup, protons were prepared by ionizing the residual H_2 gas with electrons from a field emitter array. Although the field emitter array was placed outside the cooled region, where the magnetic field was about 200 G, the electrons were injected along the magnetic field line.

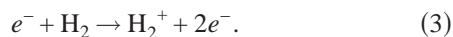
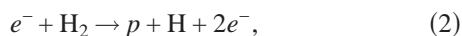
One of the ring electrodes was azimuthally segmented into four sections so that a rf electric field could be applied to compress the protons in the trap. To detect the axial oscillation of protons, a tank circuit composed of a tunable capacitor and an inductor was connected to one of the ring electrodes [10,11]. The signal was monitored by a fast-Fourier-transform (FFT) spectrum analyzer.

A microchannel plate (MCP) with a diameter of 7.5 cm combined with a phosphor screen was installed on the axis of the magnetic field about 120 cm away from the center of the trap. The mass spectra of stored ions were obtained by time-of-flight (TOF) measurements with pulsed extraction. Since the magnetic field at the MCP is ≈ 100 G, the diameter of the extracted charged particles, observed as an image on the phosphor screen, is ten times larger than that of a cloud in the trap.

III. RESULTS AND DISCUSSIONS

A. Proton energy

Protons and H_2^+ ions are produced through the following reaction processes:



The cross section of the latter process is about ten times larger than that of the former for the electron energy employed in the present study (850 eV) [12]. The initial energy distribution widths of these ions are comparable to the trap depth, i.e., ≈ 50 eV.

Protons with energy below 50 eV lose their kinetic energy via elastic scattering, vibrational excitation, and rotational excitation, which are given in Eqs. (4)–(6), respectively:

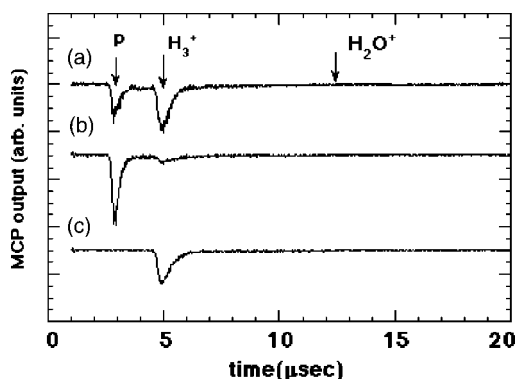
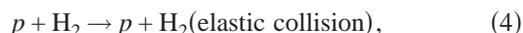
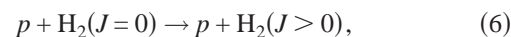
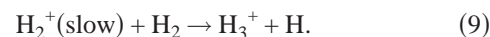
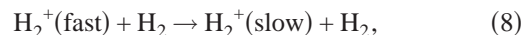


FIG. 2. Time-of-flight spectra of extracted ions with extraction energy of ≈ 800 eV. (a) Two peaks corresponding to protons and H_3^+ ions are clearly observed. (b) rf field with a frequency of 142 kHz (axial harmonic oscillation for H_3^+ ions) was applied to kick out H_3^+ ions. (c) rf field with a frequency of 248 kHz (axial harmonic oscillation for protons) was applied to kick out protons.



The cross section to form H_2^+ , the reaction denoted by Eq. (7), is about ten times less than for the other processes [13]:



The dominant atomic process of H_2^+ with an energy of 10 to 50 eV colliding with H_2 is resonant charge transfer, which yields thermal H_2^+ as given by Eq. (8). On the other hand, the dominant collision process of H_2^+ with energy less than 10 eV is H_3^+ formation as denoted by Eq. (9).

Figure 2(a) gives the TOF spectrum of extracted ions which shows that the dominant species are protons and H_3^+ ions. Although H_2^+ ions are created through reactions (3) and (7), only a small number of H_2^+ ions were detected in the TOF spectrum in Fig. 2(a). This is because H_2^+ ions were converted into H_3^+ ions as soon as they were produced [8,13]. The fraction of heavier positive ions was negligible compared with the protons and H_3^+ ions in the series of experiments. To prepare a proton cloud, H_3^+ ions were kicked out by applying a rf field of 142 kHz (f_z for H_3^+ ions with $V_0=50$ V) with an amplitude of 5 V for 10 s to the ring electrode shown in Fig. 1. Figure 2(b) shows the TOF spectrum when H_3^+ ions were selectively kicked out. The axial resonance frequency of the protons shifted higher after the rf power was turned off and approached about 248 kHz within several seconds. This is because protons with higher energy experience an unharmonic potential, which results in a lower f_z . It is suggested that the protons were thermalized due to collisions with the residual H_2 gas and resistive cooling. In the case of antiprotons, this thermalization is achieved by electron cooling. When the rf drive frequency was tuned to

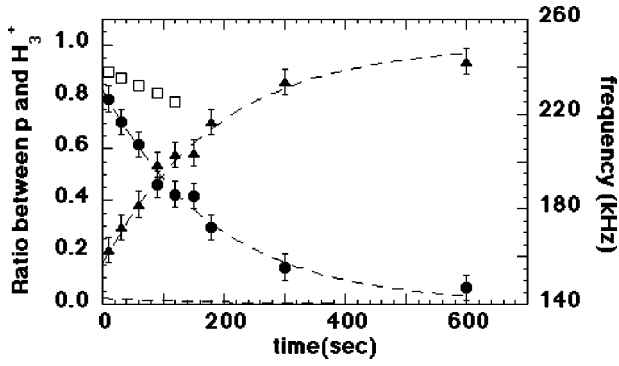


FIG. 3. The ratio between protons (solid circles) and H_3^+ (solid triangles) as a function of time. The axial resonance frequency of protons (open squares) is also plotted.

248 kHz (f_z for protons with $V_0=50$ V), protons were kicked out, keeping H_3^+ in the trap as is seen in Fig. 2(c).

The temporal evolution of ion species in the trap was studied using the prepared proton cloud. Figure 3 shows the fraction of proton (solid circles) and H_3^+ (solid triangles) as a function of storage time, which reveals that protons are converted to H_3^+ ions. Since hydrogen molecules are the major component of the residual gas, the collision processes described by the combination of Eqs. (7)–(9) are the dominant reaction channels producing H_3^+ ions from protons. The rate equations of these reactions are approximated by

$$\frac{dn_p}{dt} = -\gamma_1 n_p, \quad (10)$$

$$\frac{dn_{\text{H}_2^+}}{dt} = \gamma_1 n_p - \gamma_2 n_{\text{H}_2^+}, \quad (11)$$

$$\frac{dn_{\text{H}_3^+}}{dt} = \gamma_2 n_{\text{H}_2^+}, \quad (12)$$

where n_p , $n_{\text{H}_2^+}$, and $n_{\text{H}_3^+}$ are the densities of protons, H_2^+ ions, and H_3^+ ions, respectively. The reaction rates γ_i ($i=1,2$) are given by $\gamma_i = \sigma_i v n_{\text{H}_2}$, where v is the relative velocity between the reactant ions and molecular hydrogen. The reaction cross section σ_1 enters Eq. (7) and the effective reaction cross section σ_2 enters Eqs. (8) and (9). A least squares fitting of the experimental data yields $\gamma_1 \approx 5 \times 10^{-3} \text{ s}^{-1}$ and $\gamma_2 \approx 2 \times 10^{-1} \text{ s}^{-1}$ which result in the dashed lines in Fig. 3. Since the density of molecular hydrogen in vacuum is $n_{\text{H}_2} \approx 2.5 \times 10^7 \text{ cm}^{-3}$, the average proton energy is estimated to be ≈ 5 eV with the cross sections given in Refs. [13,14]. The estimated proton energy is much higher than the temperature of the chamber wall. It is inferred that electrical noise from the power supplies heats up the trapped ions, or the higher energy simply reflects the proton energy that has a maximum cross section for the production of H_2^+ in this energy range.

The open squares in Fig. 3 are the axial resonance frequency f_z of protons detected with the tank circuit. It is clearly seen that f_z shifts lower as the number of H_3^+ ions

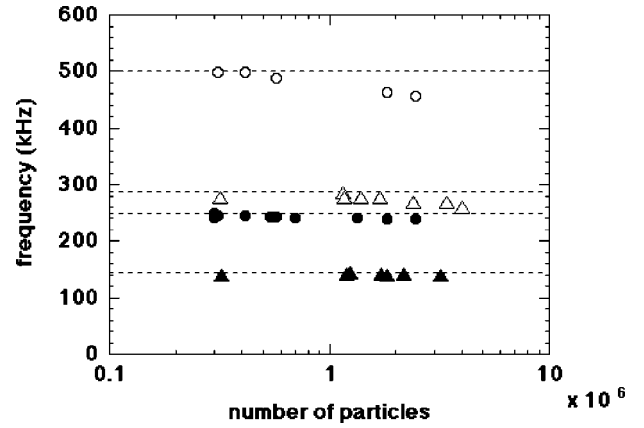


FIG. 4. The resonance frequency for the radial compression of protons (solid circles) and H_3^+ ions (solid triangles) as a function of the particle number. Open circles and open triangles correspond to the second harmonic frequencies for the radial compression of protons and H_3^+ ions, respectively. Solid circles are almost independent of the number of protons.

increases. This frequency shift is due to the additional electrostatic potential produced by H_3^+ ions which deforms the external potential $\phi_0(\rho, z)$ [15]. With the present experimental setup, the axial resonance of protons is detected until H_3^+ ions exceed 50% of the trapped ions.

B. Radial compression

The radial compression of trapped protons is important for improved extraction efficiency of the low-energy antiprotons. Radial compression of charged particles has been achieved either by sideband cooling in Penning traps or by a rotating electric field in Malmberg traps. The sideband cooling is accomplished by applying an inhomogeneous rf field at the sideband frequency $f_s = f_z + f_m$, where f_m is the magnetron frequency. Resonant heating of the axial oscillation and magnetron oscillation at f_s followed by cooling of the axial oscillation results in energy deposition to the magnetron oscillation and reduction of the magnetron radius [16]. A rotating electric field at a resonance frequency increases the angular momentum of rigid rotation of the plasma, which results in radial compression [6].

Here, a phase-shifted rf electric field was applied to the azimuthally segmented electrodes. Changing the frequency of the applied electric field, the images of extracted protons on the phosphor screen were observed. It was found that the resonance frequency of the externally applied rf for radial compression was about 243 kHz, almost independent of the number of protons ranging from 3×10^5 to 3×10^6 . The resonance width was about 2 kHz, which was probably widened due to imperfections of the applied potential $\phi_0(\rho, z)$ and the image charge effect of a large number of protons. The image of trapped protons on the phosphor screen was about 2 cm in diameter after radial compression. Considering that the magnetic field inside the trap is 100 times stronger than that at the phosphor screen, the diameter of the proton cloud was estimated to be about 0.2 cm inside the trap. In Fig. 4, the resonance frequencies for the radial

compression of proton clouds are plotted as solid circles as a function of the proton number. Also shown are the resonance frequencies for the radial compression of H_3^+ clouds (solid triangles), which are almost constant at 141 kHz. The open circles and open triangles correspond to the second harmonic frequency for the radial compression of protons and H_3^+ ions, respectively. It is seen that the second harmonic frequency depends on the number of particles. Since the number of trapped antiprotons may fluctuate shot by shot, radial compression with the fundamental resonance frequency is more favorable.

Since the magnetron frequency $f_m \approx f_z^2/2f_c$ is about 2 kHz with the cyclotron frequency $f_c \approx 15$ MHz, the frequency $f_s = f_z + f_m$ for sideband cooling of a proton is estimated to be 250 kHz theoretically. The dotted lines in Fig. 4 represent the calculated frequencies for the sideband cooling of protons (250 kHz) and H_3^+ ions (143 kHz) and their second harmonics (500 kHz and 286 kHz). Slight discrepancies exist between the theoretical and experimental values for all the resonances, probably due to small modifications of the effective potential induced by the large number of ions and small amounts of different ion species. In the present experimental conditions, it took about 100 s to compress protons with constant frequency f_s . It was observed that the conversion of protons into H_3^+ was suppressed during radial compression, which is probably due to heating up of the proton cloud. The cross section σ_1 becomes smaller at higher proton energy [13,14].

To estimate the parameters of the proton cloud before and after radial compression, the diameter of the proton cloud before the radial compression was assumed to be 2 cm, since the image of the extracted protons spread over the phosphor screen. Considering the fact that the number of protons is $\approx 10^6$ and that the proton energy is ≈ 5 eV, the axial extent of the cloud is estimated to be 4 cm for $V_0 = 50$ V. Thus, the density and Debye length of the cloud are 1.2×10^5 cm $^{-3}$ and 4.8 cm, respectively. Although the diameter of the proton cloud was ≈ 0.2 cm after compression and thermalization, the axial length remains the same, because the decisive parameter is not the density but the proton energy in the present case. The density and Debye length of the cloud were 1.2×10^7 cm $^{-3}$ and 0.5 cm after the compression. It is noted that the Debye length remains larger than the radius of the proton cloud. If the Debye length becomes much shorter than the radius of the proton cloud, it behaves as a nonneutral plasma and the frequency for the radial compression will depend on the rigid rotation frequency of the plasma [6], which is about 2 kHz before compression and 17 kHz after compression. Therefore, sideband cooling is effective for radial compression of 10^6 protons in the present experimental condition.

For the sideband cooling of antiprotons, residual H_2 gas can be harmful when its density n_{H_2} becomes high. Thus, a lower density of residual H_2 gas is favorable. In the present experiment, the residual H_2 gas contributes to the cooling of the axial motion of protons in addition to the resistive cooling. The time constant for the cooling of protons by the residual H_2 gas is estimated to be on the order of 100 s. Qualitatively, it is expected that the time necessary for the radial compression becomes longer when the residual H_2 molecules are reduced. If necessary, a small amount of elec-

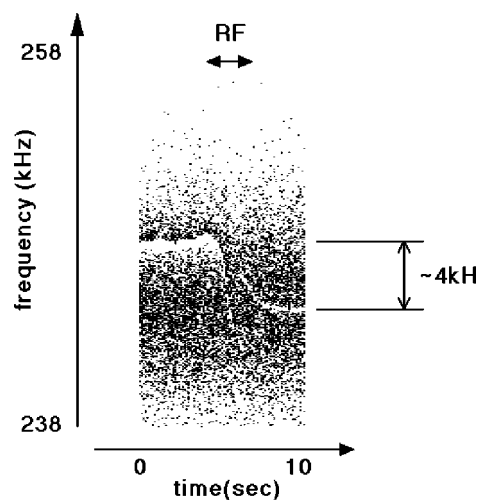


FIG. 5. A tank circuit signal with rf electric field applied for 3 s. The frequency of the externally applied rf field was swept from 150 to 250 kHz.

trons may be used in addition to the resistive cooling. In this case, the resonance frequency for the radial compression may be shifted a little.

When the rf for radial compression was swept, the compression time was drastically reduced to 3 s, which is quite short compared with the case of a fixed frequency f_s . Figure 5 shows the temporal evolution of the FFT spectrum detected by the tank circuit when the rf was swept from 150 to 250 kHz. In Fig. 5, after protons were selected inside the trap, the rf field was applied for 3 s. On applying the rf field, it was observed that the image of the extracted protons on the phosphor screen became smaller, with a diameter of 2 cm. At the same time, f_z shifts about 4 kHz lower when the proton cloud is compressed. Since the TOF spectrum showed that there were no H_3^+ ions after compression, this axial resonance frequency shift was not due to the creation of H_3^+ ions as observed in Fig. 3.

The axial resonance frequency shift associated with the radial compression can be explained as follows. The multiring trap is not designed for the precision spectroscopy of trapped particles but for the efficient electron cooling of a large number of energetic antiprotons. Therefore, there is an anharmonicity expressed by the next higher term in the Laplace expansion of the potential $\phi_1(\rho, z) = A_1(3\rho^4 - 24\rho^2z^2 + 8z^4)$ [17] in addition to the zeroth order potential $\phi_0(\rho, z) = A_0(\rho^2 - 2z^2)$. This anharmonicity shifts the axial harmonic frequency f_z as a function of the radius of the proton cloud; the shift is given by $f_z[1 + (6A_1/A_0)(r^2)_{av}]$, where $(r^2)_{av}$ is the averaged radial distribution [17]. The sign of the shift is determined by the coefficient A_1 . In the present experiment, f_z shifts 4 kHz lower when the proton cloud is compressed radially. Considering that the radius of the proton cloud is 1 cm before the compression, $A_1/A_0 \approx 3 \times 10^{-3}$ cm $^{-2}$ is estimated for the multiring trap. Although the physical explanation of this quick compression is unknown at the moment, it is very useful for the AD cycle of about 90 s.

IV. SUMMARY

Collisions of protons stored in a trap with H₂ molecules in the residual gas were studied to estimate the energy of the protons and to determine whether protons inside the trap behave as a cloud or a plasma. Proton clouds were compressed radially in the multiring trap by applying a rf field which was close to the sideband cooling frequency. When the frequency of the rf electric field for radial compression was swept, a quick radial compression of protons was observed. Since compression of $\approx 10^6$ protons was demon-

strated, the next step for the production of low-energy anti-proton beams will be the compression of $\approx 10^6$ antiprotons with resistive cooling and /or electron cooling.

ACKNOWLEDGMENTS

The authors acknowledge the support of the Cryogenic Center at Komaba, University of Tokyo. This work is supported by a Grant-in-Aid for Creative Basic Research No. (10NP0101), Ministry of Education, Science, and Culture. H.H., K.Y.F., Z.W., and M.H. are supported by JSPS.

-
- [1] Y. Yamazaki, Nucl. Instrum. Methods Phys. Res. B **154**, 174 (1999).
- [2] T. Azuma *et al.*, Report No. CERN/SPSC 97-19, 1997; Report No. CERN/SPSC P-307, 1997.
- [3] J. S. Cohen, Phys. Rev. A **56**, 3583 (1997); K. Sakimoto, *ibid.* **65**, 012706 (2002).
- [4] K. Yoshiki Franzen, N. Kuroda, H. A. Torii, M. Hori, Z. Wang, H. Higaki, S. Yoneda, B. Juhász, D. Horváth, A. Mohri, K. Komaki, and Y. Yamazaki, Rev. Sci. Instrum. **74**, 3305 (2003).
- [5] D. Wineland and H. Dehmelt, Int. J. Mass Spectrom. Ion Phys. **16**, 338 (1975); Int. J. Mass Spectrom. Ion Phys. **19**, 251 (1976).
- [6] X.-P. Huang, F. Anderegg, E. M. Hollmann, C. F. Driscoll, and T. M. O'Neil, Phys. Rev. Lett. **78**, 875 (1997).
- [7] D. J. Heinzen, J. J. Bollinger, F. L. Moore, Wayne M. Itano, and D. J. Wineland, Phys. Rev. Lett. **66**, 2080 (1991).
- [8] D. A. Church, Phys. Rep. **228**, 253 (1993).
- [9] A. Mohri, H. Higaki, H. Tanaka, Y. Yamazawa, M. Aoyagi, T. Yuyama, and T. Michishita, Jpn. J. Appl. Phys., Part 1 **37**, 664 (1998); H. Higaki, N. Kuroda, T. Ichioka, K. Yoshiki Franzen, Z. Wang, K. Komaki, Y. Yamazaki, M. Hori, N. Oshima, and A. Mohri, Phys. Rev. E **65**, 046410 (2002).
- [10] D. J. Wineland and H. G. Dehmelt, J. Appl. Phys. **46**, 919 (1975).
- [11] X. Feng, M. Charlton, M. Holtzscheiter, R. A. Lewis, and Y. Yamazaki, J. Appl. Phys. **79**, 8 (1996).
- [12] H. C. Straub, P. Renault, B. G. Lindsay, K. A. Smith, and R. F. Stebbings, Phys. Rev. A **54**, 2146 (1996).
- [13] A. V. Phelps, J. Phys. Chem. Ref. Data **19**, 653 (1990).
- [14] M. G. Holliday, J. T. Muckerman, and L. Friedman, J. Chem. Phys. **54**, 1058 (1971).
- [15] S. E. Barlow, J. A. Luine, and G. H. Dunn, Int. J. Mass Spectrom. Ion Processes **74**, 97 (1986).
- [16] D. J. Wineland, J. Appl. Phys. **50**, 2528 (1979).
- [17] R. S. Van Dyck, Jr., D. J. Wineland, P. A. Ekstrom, and H. G. Dehmelt, Appl. Phys. Lett. **28**, 446 (1976).